JOURNAL OF MATERIALS SCIENCE 31 (1996) 185–191

Investigation of microstructure of molybdenum–copper black electrodeposited coatings with reference to solar selectivity

K. M. YOUSIF, B. E. SMITH
Department of Mechanical Engineering, Brunel University, Uxbridge UB8 3PH, UK
C. JEYNES
Department of Electronic and Electrical Engineering, Surrey University, Guildford GU2 5XH, UK

Optical and microstructural properties of electrodeposited molybdenum–copper (Mo–Cu) black coatings have been studied with reference to their selectivity in absorption of solar radiation. Such coatings were found to have a solar absorptance, α, about 0.87 and low thermal emittance, ε, such that the selectivity, α/ε, was 3.6. Electrodeposited molybdenum-black coatings generally have selectivity $\alpha/\varepsilon \sim 3$. The oxidation state of molybdenum in (Mo–Cu) black coatings as determined by X-ray photoelectron spectroscopy is about +5 (which is fairly close to that of Mo_4O_{11}). Large numbers of irregular particles were found on the surface of molybdenum–copper black coatings. There is evidence that the particles contain copper oxide.

1. Introduction

Efficient conversion of solar energy into thermal energy (e.g. in heating of media such as water) requires selective absorber surfaces which have high solar absorptance, α, and low thermal emittance, ε. A large number of selective coatings has been developed [1–5] many of which are based on black metallic oxides.

Molybdenum black coatings have been the subject of a number of investigations related to their possible use as a solar selective absorbers [6–19]. Solar absorptance and thermal emittance values of electrodeposited molybdenum black coatings indicate that their selectivity is rather low. This is due to their high emittance, which is probably related to relatively high coating thickness. Molybdenum black dip coatings are usually thinner and generally much more spectrally selective [13].

In this work, some attempts have been made to improve the selectivity of electrodeposited molybdenum black coatings by addition of copper. Potdar *et al.* [11] added $CuSO_4$ to their plating solution for molybdenum black $\{(NH_4)_2MoO_4\}$. In this investigation, $CuSO_4$ was added to a plating bath of the electrolyte ammonium paramolybdate $\{(NH_4)_6Mo_7O_{24}\cdot 4H_2O\}$.

2. Experimental procedure

2.1. Sample preparation

Copper sheet was mechanically polished with emery paper to remove the oxide layer, and washed with distilled water. It was then chemically polished [18], cleaned, and dried. This was followed by immersion in a plating tank for electrodeposition of a nickel intermediate layer which was usually dull but sometimes bright nickel. Molybdenum–copper (Mo–Cu) black coatings were produced on the resulting substrate by electrodeposition with small amounts ($2.5\,g\,l^{-1}$) of $CuSO_4$ in the plating bath. The operating conditions and the concentration of the plating bath were selected after investigating the effects of the following parameters: pH, temperature, current density, plating time, concentrations of copper sulphate, ammonium paramolybdate, and boric acid. A Hull cell was used for this purpose [18].

2.2. Radiative properties

Both solar absorptance and thermal emittance values of the coating samples were determined from spectral reflectance measurements by application of Kirchoff's law for an opaque surface. The solar absorptance, α, of coating samples was determined by measuring their total spectral reflectance, diffuse (ρ_d) + specular (ρ_s), in the wavelength range 0.30–2.5 μm. A Perkin–Elmer (Lambda-9) spectrophotometer, equipped with an integrating sphere of diameter 60 mm was used to measure either the total or diffuse reflectance. A barium sulphate tile was used as a standard white reference sample. The specular reflectance of the coating samples in the infrared region (2.5–50 μm) was obtained by using a Perkin–Elmer (model 683) double-beam recording spectrophotometer with a reflectance attachment.

The solar absorptance, α, of the coatings was calculated from their total reflectance data in the solar region using the selected ordinate method [20]. This

0022–2461

was done for the air mass 2 (AM2) solar spectrum, given by Wiebelt and Henderson [21]. To calculate the thermal emittance, ε, the specular reflectance values were weighted, using the Planck radiation distribution formula [20], as calculated by Sargent [22] for a solar absorber operating temperature of 313 K.

2.3. Surface analysis of the coatings

The topography of the coatings was examined using scanning electron microscopy (SEM) with a Cambridge Stereoscan S250. Energy dispersive X-ray analysis (EDX) was carried out using the same instrument (this was equipped with a silicon solid state X-ray detector and a Link system (model 860) for qualitative and quantitative analysis). X-ray diffraction patterns were obtained with a Philips PW 1729 diffractometer, controlled by a PW1710 unit. A copper target was used to generate CuK_α radiation (0.15405 nm). X-ray photoelectron spectroscopy (XPS) spectra were recorded using a Kratos (model ES 300) spectrometer. The AlK_α line (1486.6 eV) was used as the X-ray excitation source. The resolution of this instrument is $\pm$ 0.95 eV. Analysis of (Mo–Cu) black coatings by the ion-beam (IB) technique, or Rutherford back-scattering (RBS) spectrometry was carried out using an ion source producing charged particles accelerated by a Van de Graff generator to mega electron volt energies. Two different sorts of beams were employed (proton and helium ions). The proton beam (H^+) having an energy of 1.670 MeV, was used to penetrate deeply into the sample and to give a high sensitivity for detection of oxygen. To investigate the proportions of various metals near the surface, a 1.50 MeV helium ion beam ($^4He^+$) was used (this equipment is located at Surrey University).

2.4. Evaluation of surface roughness

The measurement of roughness was taken as the roughness average value designated R_a and expressed in micrometres. This is the arithmetical average value of the deviation of the surface profile from a reference line (throughout the prescribed sampling length) [23] taking all deviations as positive. The roughness of the coatings was measured using a Talysurf apparatus (Rank-Taylor-Hobson Talystep).

3. Results

3.1. Radiative properties

The total reflectance spectra of the (Mo–Cu) black coatings on nickel-plated copper substrates show that the coatings have relatively low reflectance in the visible region. Interference peaks were observed in the reflectance spectra of the coatings prepared with deposition times in the ranges 20–120 s.

To illustrate the effect of increasing the coating thickness upon the radiative properties, α and ε are plotted as functions of the coating mass per unit area (W/A) in Fig. 1. Both α and ε increase with coating thickness. Plating times in the range 120–140 s were selected as giving optimum values of α and ε on the basis of these results.

Coating thicknesses were determined using ion beam analysis and study of optical interference peaks in reflectance curves. The estimated thickness for the (Mo–Cu) black coating was about 0.8 μm (when the deposition time was 120 s, and the current density was 4 mA cm^{-2}), while the estimated thickness for the molybdenum black coating was about 1 μm (when the deposition time was 120 s, and the current density was 3.5 mA cm^{-2}).

The (Mo–Cu) black coatings have somewhat better optimum selectivity ($\alpha/\varepsilon = 3.6$, when $\alpha = 0.87$), than that of electrodeposited molybdenum black coatings ($\alpha/\varepsilon = 3.1$, when $\alpha = 0.73$). It was found that optimum α/ε for (Mo–Cu) black coatings increased to about 5 for an α value of 0.87 when a bright nickel intermediate layer was used instead of a dull nickel intermediate layer.

3.2. Surface analysis of the coatings

3.2.1. SEM and EDX

Electroplated molybdenum black coatings on nickel-plated copper-substrates have microstructures of relatively flat irregular platelets, separated by prominent fissures (Fig. 2). EDX tests were carried out in two

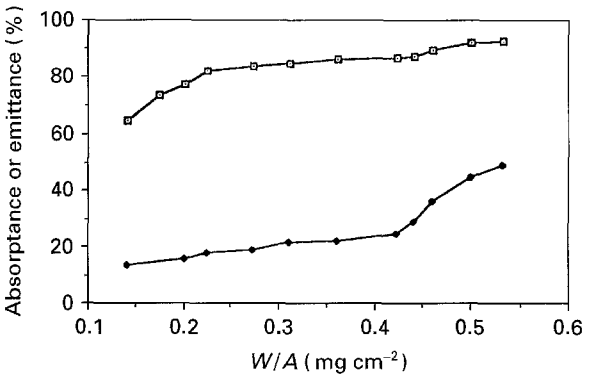

Figure 1 Variation of (□) solar absorptance, α, and (◆) thermal emittance, ε, with the coating mass per unit area (W/A) for electrodeposited (Mo–Cu) black coatings.

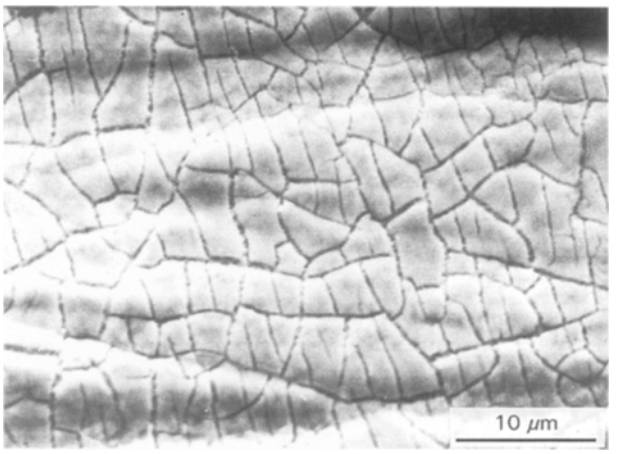

Figure 2 Scanning electron micrograph of an electrodeposited molybdenum black coating on a Ni/Cu substrate. Time of deposition = 120 s.

regions of the molybdenum black coatings: the film areas and crack areas. The corresponding EDX spectrum is shown in Fig. 3. This shows that the coating consists mainly of molybdenum and a smaller proportion of nickel, as well as a small amount of copper, which may come from the copper substrate. Because the detector of the EDX system had a thin beryllium window, X-rays from elements with atomic numbers of less than 11 (such as oxygen) were not detectable. Coating compositions (at %) determined by EDX are given in Table I.

The stages in film growth of (Mo–Cu) black coating on Ni/Cu substrates after various electrodeposition times were monitored using SEM. For the first stage of electrodeposition (e.g. electrodeposition time ~ 30 s), the surface topography includes roughly spherical particles. The coatings have irregularly shaped particles, on the surface (Fig. 4) after a deposition time of 120 s. The corresponding EDX spectrum (Fig. 5) indicates that the coating consists mainly of molybdenum and nickel with copper (Table I).

3.2.2. X-ray diffraction

An X-ray diffraction (XRD) pattern of an electroplated (Mo–Cu) black coating on a Ni/Cu substrate is shown in Fig. 6. A weak diffraction peak has been observed with maximum intensity between $\theta = 4.5°$ and 5.5°. The corresponding lattice spacing is 0.8182 nm. To ensure that this peak is due to the coating and not to the Ni/Cu substrate or instrumentation, the diffraction pattern for an uncoated Ni/Cu substrate was also obtained. No peak was then observed.

3.2.3. XPS

The carbon C(1s) peak has been used as a reference peak for determination of electron binding energies by X-ray photoelectron spectroscopy (XPS). The binding energy (BE) of the C(1s) peak was found to be 284.9 eV by calibration of the spectrometer according to Anthony and Seah [24].

The oxidation states of molybdenum black and (Mo–Cu) black coatings were estimated by comparing the BE (from the XPS spectra) with those of standard molybdenum metal foil, MoO_3, and other molybdenum oxides (Table II). MoO_3 powder was supplied by BDH Chemical Ltd (purity 99.5%). MoO_2 powder was supplied by Alfa-Ventron (purity 99%). A typical survey scan XPS spectrum of an as-prepared (Mo–Cu) black coating on a Ni/Cu substrate is given in Fig. 7. It shows that the coating consists mainly of molybdenum and other elements like nickel and copper together with oxygen. It is thought that the nickel and copper signals are mainly from the coating (not the substrate) because the average depth of XPS analysis is in the range 1.5–3.0 nm

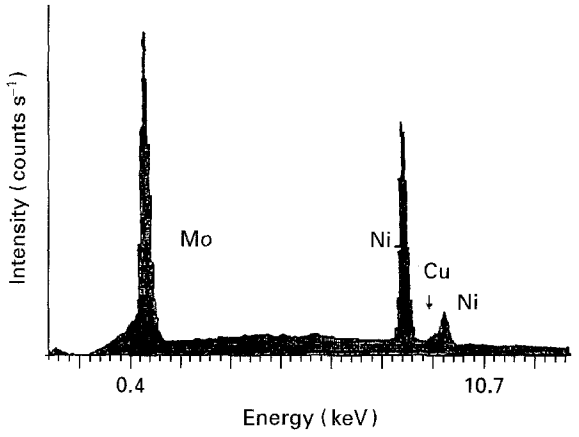

Figure 3 EDX spectrum from the surface of the electrodeposited molybdenum black coating on a Ni/Cu substrate (of Fig. 2).

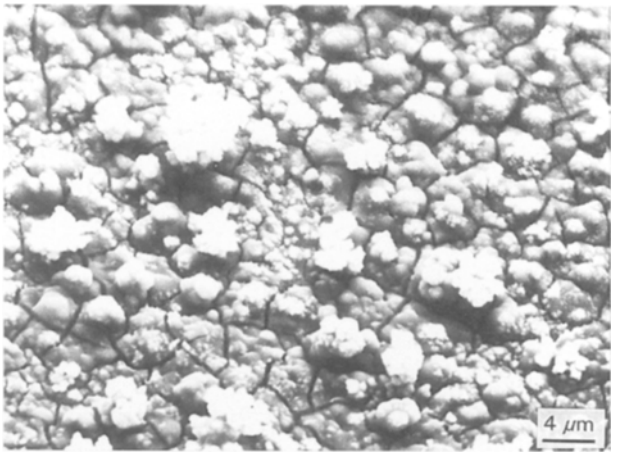

Figure 4 Scanning electron micrograph of electrodeposited (Mo–Cu) black coating on a Ni/Cu substrate. Time of deposition = 120 s.

TABLE I Composition of electrodeposited molybdenum black coatings, obtained by EDX

Sample	Tested area[a]	Mo (at %)	Ni (at %)	Cu (at %)
Electrodeposited molybdenum black coating	F	65.3	9.5	25.2
on copper substrate (t = 5 min)	C	39.2	7.8	52.7
Electrodeposited molybdenum black coating	F	55.4	42.7	1.9
on Ni/Cu substrate (t = 2.5 min)				
Electrodeposited (Mo–Cu) black coating	F	8	88.6	3.4
on Ni/Cu substrate (t = 30 s)				
Electrodeposited (Mo–Cu) black coating	F	34.4	32.9	32.8
on Ni/Cu substrate (t = 120 s)	P	18.9	7	74.1
Electrodeposited (Mo–Cu) black coating	F	38.8	23.1	38.1
on Ni/Cu substrate (t = 150 s)	C	32.9	35.5	20.4

[a] F = film area, C = crack area, P = particle area.

[25]. The appearance of the C(1s) peak in the XPS spectra originates from the spectrometer rotary pump oil that inevitably contaminates the samples at the working pressure ($\sim 10^{-5}$ Pa). Fig. 8 shows the Mo-3d doublet and the O(1s) peak. The O(1s) peak is almost symmetrical. The Cu(2p) and Ni(2p) peaks, are accompanied by satellite peaks which suggests they are both present as oxides. The values of BE for $Mo(3d_{3/2}-3d_{5/2})$ electrons and other chemical elements present in (Mo–Cu) black coatings are shown

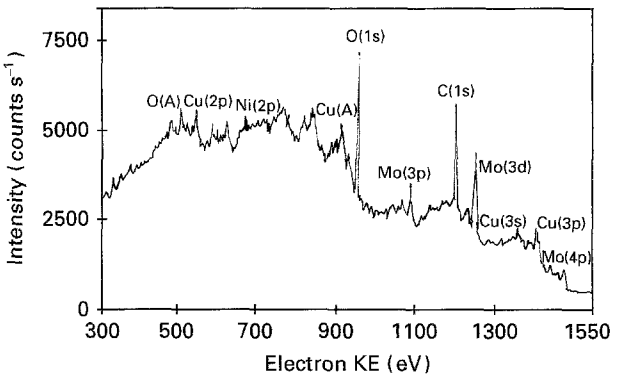

Figure 7 Survey scan of XPS spectrum of an electrodeposited (Mo–Cu) black coating on Ni/Cu substrate.

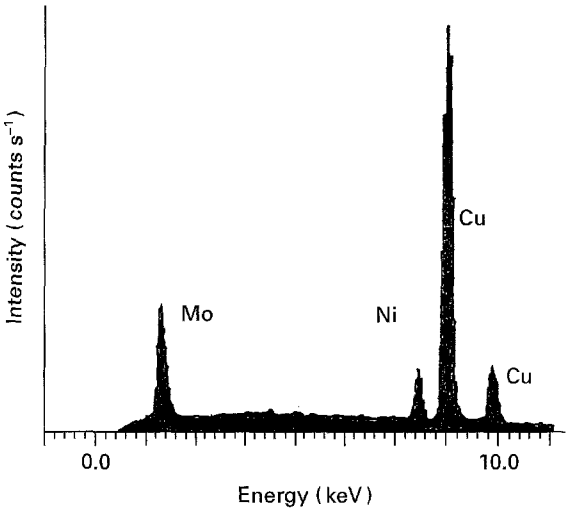

Figure 5 EDX spectrum from the surface of the electrodeposited (Mo–Cu) black coating (of Fig. 4).

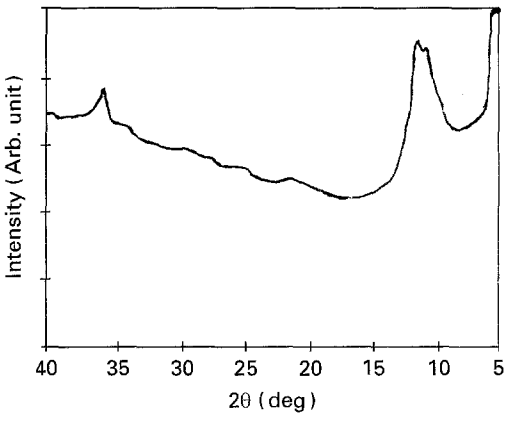

Figure 6 X-ray diffraction pattern (CuK_α) of an electrodeposited (Mo–Cu) black coating on Ni/Cu substrate.

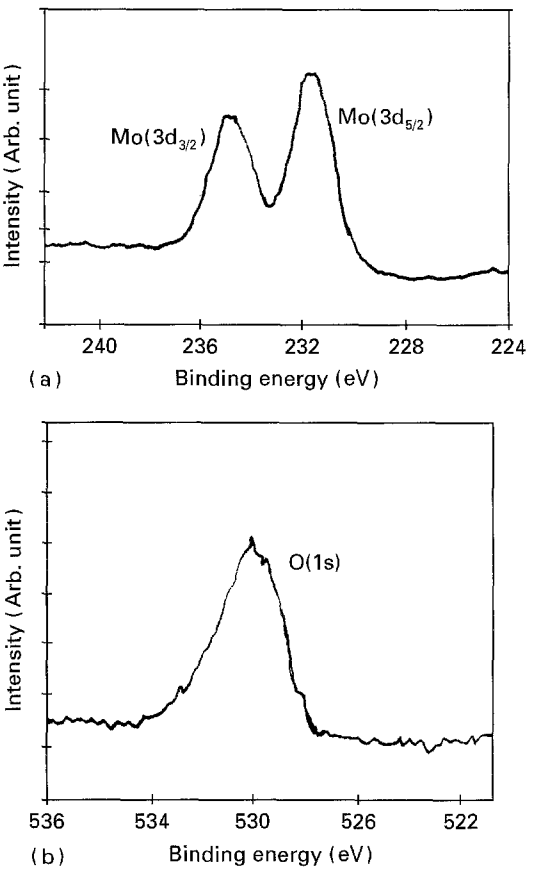

Figure 8 Narrow scan of XPS spectra of a (Mo–Cu) black coating on Ni/Cu substrate. (a) Mo(3d) doublet, (b) O(1s) peak.

TABLE II XPS data for standard samples, including shift in binding energy of Mo 3d5/2 peak with respect to that of Mo 3d5/2 peak of molybdenum metal together with corresponding oxidation state

	Electron binding energy[a] (eV)				FWHM for Mo (3d5/2) (eV)	Shift in BE of Mo (3d5/2) (eV)	Oxidation state
	Mo (3p3/2)	Mo (3d3/2)	Mo (3d5/2)	O(1s)			
Molybdenum metal	–	230.7	227.5	–	1.9	0	0
MoO_3	398.6	236.5	233.4	530.3	2.1	5.9	[+6]
MoO_2	396	232.9	229.8	530.4	–	2.3	[+4]
$MoCl_2$[b]	–	234.5	231.5	–	–	4	[+5]

[a] The associated error in these measurements = ± 0.20.
[b] Data taken from Swartz and Hercules [32].

TABLE III XPS data for an electrodeposited (Mo–Cu) black coating on a Ni/Cu substrate, including shift in binding energy of Mo 3d5/2 peak with respect to that of molybdenum metal[a]

Electron binding energy[b] (eV)						FWHM for Mo (3d5/2) (eV)	Shift in BE of Mo (3d5/2) (eV)
Mo (3p3/2)	Mo (3d3/2)	Mo (3d5/2)	O(1s)	Ni (2p3/2)	Cu (2p3/2)		
397.6	234.6	231.6	530	856.8	932.5	2	4.1

[a] Mo (3d5/2) for molybdenum metal = 227.5 eV.
[b] The associated error in these measurements $\simeq \pm 0.20$ eV.

TABLE IV Atomic percentage composition of a (Mo–Cu) black coating, on a Ni/Cu substrate, determined by XPS

Mo	O	Ni	Cu
20.3	67.3	4.4	8

in Table III together with the full-width at half-maximum (FWHM) value, for the Mo($3d_{5/2}$) peak, together with the shift in BE of the Mo($3d_{5/2}$) peak from that of Mo metal. The estimated accuracy in this method is ± 0.2 eV [26]. The composition of the coatings has been determined by measuring the photoelectron peak areas of the individual constituent elements and then dividing by their corresponding sensitivity factors [18]. The resulting atomic percentages of chemical elements present in electrodeposited (Mo–Cu) black coatings, are given in Table IV.

3.2.4. Ion-beam analysis

Ion-beam (or Rutherford back-scattering, RBS) analysis provides the ability to distinguish the atomic masses of elements and their distribution in depth as a function of detected energy. A typical back-scattering (BS) spectrum of an electroplated (Mo–Cu) black coating on a Ni/Cu substrate is shown in Fig. 9. In this figure, back-scattering yield (number of particles counted by the detector) is plotted as a function of channel number. Typical results for the resulting composition of a (Mo–Cu) black coating, are given in Table V.

3.2.5. Evaluation of surface roughness

The surface topography of the coatings depends upon the pretreatment of the substrate, as well as the composition and deposition conditions of the coatings. Surface roughness could affect the emittance of the surface, e.g. a highly polished substrate will tend to have a lower emittance (due to higher reflectance) than that of a rough surface. It could also lead to enhanced absorptance due to multiple reflections within surface cavities having dimensions of the order of solar wavelengths. The surface profile stylus used in the roughness measurements had a tip radius of 2.5 μm, hence only features coarser than this could be detected. The central line average roughness (CLA) values of the (Mo–Cu) black coatings was about 0.65 μm, while that of the molybdenum black coatings was about 0.5 μm.

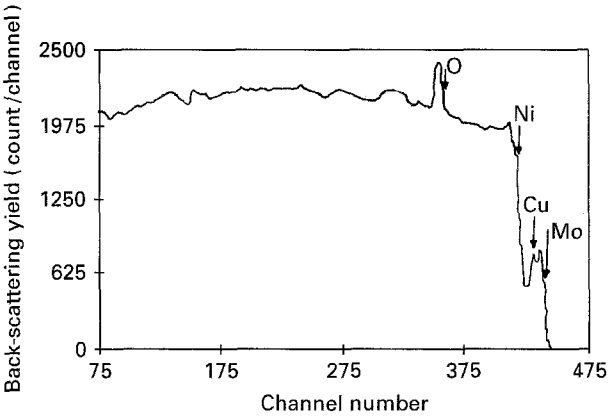

Figure 9 Ion back-scattering spectrum ($\theta = 160°$) for an electrodeposited (Mo–Cu) black coating and 1.67 MeV H ions.

TABLE V Atomic percentage composition of a (Mo–Cu) black coating, on a Ni/Cu substrate, determined by ion beam analysis (M = Cu + Ni)

Mo	O	(M)
11.6	57	31.4

4. Discussion

4.1. Radiative properties of (Mo–Cu) black coatings

The plating time has a pronounced effect on the optical properties of the coatings. As the thickness of the coating increases, both α and ε increase due to reflectance decreases in both the visible and infrared portions of the spectrum. The high absorptance of these coatings may be related to optical interference for the thinner coatings The semiconducting nature of the molybdenum black coatings [14] is thought to contribute to their selectivity. Further work would be required to establish whether or not (Mo–Cu) black coatings are also semiconductors.

4.2. Characterization of as-prepared coatings

4.2.1. Micromorphology

The surface topography of molybdenum black coatings electrodeposited on Ni/Cu consists of rather smooth and flat platelets with large and deep cracks. A scanning electron micrograph cross-section of these coatings, indicates the presence of cracks and probably some micro-voids in the coatings. The formation of the cracks, may be due to loss of some

water from the coating [17], or due to heat produced by electron bombardment. The other reason for cracking may be related to the thermal expansion mismatch between the coating material and the substrate [27]. The surface topography of electrodeposited (Mo–Cu) black coatings is more complex than that of electrodeposited molybdenum black coatings, i.e. irregular particles appear on the surface of the coating and are distributed randomly (Fig. 4). The uniformity of coating thickness is dependent on the electro-deposition conditions. As the thickness of this coating increases, the surface appears smoother and flatter. The surface topography of coatings depends upon the pretreatment of the substrate as well as the composition and deposition conditions of the coatings. Central line average roughness (CLA) values, indicate that these coatings are rather rough. The roughness of the substrate, and/or intermediate layers could affect the optical properties (i.e. the reflectance), and therefore α and ε of the overlay surface (molybdenum black coating).

4.2.2. Compositional and structural analysis

EDX compositional analysis of electrodeposited (Mo–Cu) black coatings on Ni/Cu substrates shows that the coating apparently consists mainly of molybdenum, copper and nickel (Table I). Some of the copper and nickel signals are probably related to substrates. These signals appear through cracks or through the coating itself. The irregular particles on the surface of (Mo–Cu) black coatings are rich in copper oxide (according to XPS analysis). Qualitative and quantitative analyses by XPS for electrodeposited (Mo–Cu) black coatings on Ni/Cu substrates, shows that these coatings consists mainly of oxygen (66%–67%), together with molybdenum and small amounts of nickel hydroxide and copper oxide [18].

The X-ray diffraction study for an as-prepared electroplated (Mo–Cu) black coating, yielded a broad low-angle peak with maximum intensity between $\theta = 4.5°$ and 5.5°. The result is similar to that obtained by Jahan [13], where a peak at about 4.7° was observed and was identified as the 200 diffraction peak of Mo_4O_{11}. The absence of other peaks of Mo_4O_{11} may be due to preferred orientation of Mo_4O_{11} in the coating relative to the substrate.

Rutherford back-scattering (RBS) for electroplated (Mo–Cu) black coatings on Ni/Cu substrates indicates that the coating consists mainly of oxygen together with molybdenum, nickel and copper (Table V).

The discrepancies in coating compositions between those determined by RBS and those obtained by other techniques, such as XPS and EDX (Table I), may be due to depth variation in composition of the coatings. The surface sensitivity and depth resolution of these techniques may contribute to the above discrepancies. The analytical range in RBS is from $Z = 1$ (H) to $Z = 92$ (U), while in the EDX technique used in this study, the range is from $Z = 11$ (Na) to $Z = 92$ (U), i.e. oxygen could not be detected by EDX. The penetration depth in RBS is 1–2 μm, while in EDX it is up to 5 μm, and in XPS it is in the range 15×10^{-4} to 30×10^{-4} μm [28, 29]. The proportion of copper and nickel appears to increase with depth below the coating surface, according to a comparison of the XPS and ion-beam results in Tables IV and V, respectively. This may, however, be due to the substrate materials.

According to the XPS study, it is observed that the shift in BE from molybdenum metal was 4.2 eV, and this indicates that the oxidation state is about + 5. This oxidation state is fairly close to the oxidation state of Mo_4O_{11} (+ 5.5) [30, 31]. Potdar *et al.* [10] reported that a similar coating on a nickel-plated copper substrate, consists of the MoO_3 phase. It is clear that these results are not supported by the present study.

In summary, electrodeposited (Mo–Cu) black coatings are rich in copper (which could be a mixture of metallic and oxide phases) and molybdenum oxide (Mo_4O_{11}) (according to XRD and XPS) together with $Ni(OH)_2 \cdot Cu_2O$, (according to XPS) and H_2O.

5. Conclusions

Electrodeposited molybdenum black coatings have an optimum selectivity factor, $\alpha/\varepsilon = 3.1$, when $\alpha = 0.73$. (Mo–Cu) black coatings (deposited on dull nickel) have an optimum selectivity factor, $\alpha/\varepsilon = 3.6$ (when $\alpha = 0.87$), and when deposited on a bright nickel have α/ε of 5 (when $\alpha = 0.87$).

The microstructure of molybdenum black electrodeposited coatings, consists of relatively flat, smooth, irregular platelets with prominent fissures. The coatings of (Mo–Cu) black, have irregular shaped particles on the surface. Both molybdenum black and (Mo–Cu) black coatings, mainly consist of Mo_4O_{11}, together with a small percentage of nickel, possibly in the form of a hydroxide. Cuprous oxide is present in (Mo–Cu) black coatings and is thought to be associated with prominent irregular particles on the surface of these coatings.

Acknowledgments

We wish to thank Dr J.K. Critchley, Chemistry Department, Surrey University, for provision of laboratory facilities, and valuable discussions. We are most grateful to Dr R. Bulpett and his colleagues of the Experimental Techniques Centre at Brunel University, for useful discussions and experimental assistance with SEM, EDX and XPS.

References

1. G. A. NIKLASSON and C. G. GRANQVIST, *J. Mater. Sci.* **18** (1983) 3475.
2. W. F. BOGAERTS and C. M. LAMPERT, *ibid.* **18** (1983) 2847.
3. O. P. AGNIHOTRI and B. K. GUPTA, "Solar Selective Surfaces" (Wiley, New York, 1981).
4. S. A. HERZENBERG and R. SILBERGLITT in *Proc. Society of Photo Optical Instrumentation Engineers*, **324** (International Society for Optical Engineering, Bellingham, Washington, 1982) 92.
5. C. M. LAMPERT, in "Advances in Solar Energy", Vol. 5, edited by K. W. Boer (Plenum Press, 1989).
6. G. E. CARVER, *Solar Energy Mater.* **1** (1979) 357.

7. E. E. CHAIN and B. SERAPHIN, *Thin Solid Film* **123** (1985) 197.
8. B. E. SMITH, R. HOSSEINI, C. FARMAKIS and J. K. CRITCHLEY, in "Proceedings of Solar World Forum", edited by D. O. Hall and J. Morton (Pergamon Press, Oxford, 1982) p. 226.
9. F. JAHAN and B. E. SMITH, *J. Mater. Sci.* **27** (1992) 625.
10. H. S. POTDAR, R. I. HEGDE, S. BADRINARAYAN and NEETA PAVASKAR, *Solar Energy Mater.* **6** (1982) 183.
11. H. S. POTDAR, A. B. MANDALE, S. D. SATHAYE and A. P. B. SINHA, *J. Mater. Sci.* **22** (1987) 2023.
12. F. JAHAN and B. E. SMITH, *J. Mater. Sci. Lett.* **5** (1986) 905.
13. F. JAHAN, PhD thesis, Brunel University (1987).
14. F. JAHAN and B. E. SMITH, *Solar Energy Mater.* **20** (1990) 215.
15. R. HOSSEINI, PhD thesis, Brunel University (1981).
16. R. HOSSEINI, B. E. SMITH and J. K. CRITCHLEY, *J. Surf. Technol.* **20** (1983) 321.
17. K. M. YOUSIF and B. E. SMITH, in "Energy and the Environment Into the 1990s", Procedings of the 1st World Renewable Energy Congress, Reading, 23–28 Sept. 1990, edited by A. M. Sayigh, Vol. 3 (Pergamon Press, Oxford, 1990) p. 1383.
18. K. M. YOUSIF, PhD thesis, Brunel University, (1992).
19. K. M. YOUSIF, B. E. SMITH and C. JEYNES, in "Energy and the Environment into the 1990s", Proceedings of the 3rd World Renewable Energy Congress, Reading, UK, 11–16 September 1994, edited by A. A. M. Sayigh, Vol. 5(1) (Pergamon, Elsevier Science, 1994) p. 324.
20. J. A. DUFFIE and W. A. BECKMAN, "Solar Engineering of Thermal Processes", 2nd Edn (Wiley, New York, 1991).
21. J. A. WIEBELT and J. B. HENDERSON, *J. Heat Transfer* **101** (1979) 101.
22. S. L. SARGENT, *Bull. Am. Meteorol. Soc.* **53** (1979) 360.
23. H. DAGNALL, "Exploring Surface Texture" (Rank Taylor Hobson, Leicester, UK, 1980).
24. M. T. ANTHONY and M. P. SEAH, *Surf. Interface Anal.* **6** (1984) 107.
25. J. C. RIVIERE, in "Surface Analysis of High Temperature Materials: Chemistry and Topography", edited by G. Kemeny (Elsevier Applied Science, London, 1984) p. 91.
26. D. BRIGGS and M. P. SEAH, "Practical Surface Analysis by Auger and X-ray Photoelectron Spectroscopy", 2nd Edn (Wiley, Chichester, 1990).
27. B. M. KRAMER, *Thin Solid Films* **108** (1983) 117.
28. L. C. FELDMAN and J. W. MAYER, "Fundamentals of Surface and Thin Film Analysis" (North-Holland, London, 1986).
29. J. M. WALLS, "Methods of Surface Analysis" (Cambridge University, Cambridge, 1989).
30. M. J. KENNEDY, PhD thesis, Brunel University (1972).
31. T. H. FLEISCH and G. J. MAINS, *J. Chem. Phys.* **76** (1982) 780.
32. W. E. SWARTZ and D. M. HERCULES, *Anal. Chem.* **43** (1971) 1774.

Received 11 July 1994
and accepted 15 August 1995